

Tests of gravitational wave propagation with LIGO-Virgo catalog

Xian-Liang Wang^{1,2,3}, Shu-Cheng Yang⁴, and Wen-Biao Han^{4,1,3*}

¹*School of Fundamental Physics and Mathematical Sciences,
Hangzhou Institute for Advanced Study,
UCAS, Hangzhou 310024, China*

²*Institute of Theoretical Physics,
UCAS, Beijing 100190, China*

³*University of Chinese Academy of Sciences,
100190 Beijing, China*

⁴*Shanghai Astronomical Observatory,
Shanghai 200030, China*

(Dated: January 7, 2025)

In the framework of general relativity (GR), gravitational waves (GWs) travel at the speed of light across all frequencies. However, massive gravity and weak equivalence principle (WEP) violation may lead to frequency-dependent variations in the propagation speed of GWs, which can be examined by comparing the theoretical and observed discrepancies in the arrival times of GW signals at various frequencies. This provides us with an opportunity to test these theories. For massive gravity, we consider that gravitons may have a nonzero rest mass. For WEP violations, we hypothesize that different massless particles exposed to the same gravitational source should exhibit varying gravitational time delays. The gravitational time delay induced by massive gravitational sources is proportional to $\gamma + 1$, where the parameter $\gamma = 1$ in GR. Therefore, we can quantify these two deviations using phenomenological parameters m_g and $|\Delta\gamma|$, respectively. In this study, we use selected GW data from binary black hole coalescences in the LIGO-Virgo catalogs GWTC-2.1 and GWTC-3 to place constraints on the parameters m_g and $|\Delta\gamma|$. We analyze the relationship between m_g and luminosity distance, as well as between $|\Delta\gamma|$ and both luminosity distance sky location of GW events to determine the presence of graviton mass and WEP violation. Nevertheless, we find no evidence of such relationships. We also compute Bayes factors for models that assume the existence of graviton mass and WEP violation compared to the standard GW model, respectively. The absolute value of the natural logarithm of the Bayes factor is generally less than 2. Our analysis reveals no significant preference for either model. Additionally, the Bayes factors between these two models do not provide obvious evidence in favor of either one.

I. INTRODUCTION

The detection of gravitational waves (GWs) by LIGO [1] and Virgo [2] collaborations heralds a new era in both astrophysics and fundamental physics [3–8]. During the third observing run (O3), Advanced LIGO, Advanced Virgo and KAGRA added 79 GW events, as detailed in GWTC-2.1 [7] and GWTC-3 [8]. These discoveries deepen our understanding of the universe and provide powerful tools to check the rules of gravitational theories such as general relativity (GR), and help us better understand the basic structure of spacetime.

According to GR, GWs are theorized to propagate at the speed of light in a vacuum, and their velocity v_g is predicted to be invariant across all frequencies. This characteristic suggests that the propagation speed of GWs is unaffected by frequency, ensuring uniformity in the velocity across different wavelengths. The GWs detected by Advanced LIGO and Advanced Virgo can be used to make statistical inferences about v_g [9–12], and the speed of GWs can be constrained within the range of $0.99^{+0.01}_{-0.02}c$ at a 90% credible interval [11]. In the

framework of the quantum gravity theory, gravitons are postulated to be carriers for transmitting gravitational interactions. GWs travel at the speed of light across all frequencies which supports the idea that gravitons are massless.

However, certain modified gravitational theories typically anticipate violations of Lorentz invariance (LI) [13–20], indicating that the speed of GWs might not always align with the speed of light and could vary based on their frequencies during propagation [21–24]. These theories imply that gravitons may possess a rest mass that is not equal to zero. We use modified dispersion relations to depict these theories [26], and we focus our discussion on a specific scenario, which is the massive gravity [25]. It is hypothesized that low-frequency GWs propagate slower than high-frequency GWs. Consequently, during the inspiral phase of compact binary stars, gravitons emitted earlier have a lower propagation speed than those emitted later. This phenomenon induces phase alterations in GWs during propagation, resulting in received waveforms that differ from those predicted by GR. If such dephasing of waveforms comparing with GR's templates is not detected, this could imply a constraint on the graviton mass, thereby limiting the potentially extent of LI violation. The graviton mass has been measured through

* wbhan@shao.ac.cn

various experimental datasets[27–32].

Similar to the impact of the massive gravity, if the weak equivalence principle (WEP) is violated, the speed of GWs will no longer be the speed of light but will depend on the frequencies. This frequency dependence allows us to limit the extent of WEP violation. The violation of WEP results in different Shapiro delays [33] for different massless particles traversing an identical gravitational field. The Shapiro delay is proportional to $\gamma + 1$, where γ is the parametrized post-Newtonian parameter ($\gamma = 1$ in general relativity) [34, 35], and different massless particles will have different values of γ during free fall in a gravitational field if WEP is violated. It is often considered that two different massless particles are emitted from the same astrophysical source, with respective values of γ_1 and γ_2 , then $|\Delta\gamma|$ ($|\gamma_1 - \gamma_2|$) can be used to quantitatively represent the violation of the WEP. If we know the intrinsic time delay of these two particles, we can limit the difference in the Shapiro time delay between the two particles Δt_{gra} [36] which is proportional to $|\Delta\gamma|$, by measuring the observed time-delays Δt_{obs} . Therefore, we can establish an upper limit for $|\Delta\gamma|$ by observing the Δt_{obs} of various signals emitted from the same source. Several constraints on $|\Delta\gamma|$ have been derived from various astrophysical events, including the emissions from the supernova event SN1987A [36, 37], gamma-ray bursts [38–43] and fast radio bursts (FRBs) [44–47]. In this study, we use GWs to test WEP, which had previously been employed [48–51]. The utilization of GW signals can eliminate the intrinsic time delay when signals are emitted, which will enable us to estimate the up-limit of $|\Delta\gamma|$ more accurately.

Building on the previously discussed framework, we further explore the phenomena of massive gravity and WEP violation, both of them modify the speed of GWs resulting in frequency dependence. Specifically, if gravitons possess mass, the speed of gravitons emitted during the early inspiral phase of GW emission is expected to be lower than that emitted later. Consequently, the impact of this effect on the GW waveform is expected to become more pronounced as the luminosity distance of GW events from Earth increases. This is consistent with the behavior under WEP violation, where the influence of gravitational fields leads to cumulative effects as the luminosity distance of the GW increases. However, it is essential to note that WEP violation manifests through changes in the speed of GWs due to the influence of gravitational fields.

In this study, our analysis focuses on the gravitational potential generated by the Milky Way, under the assumption that its entire mass is concentrated at the center. Owing to the unclear details of the host galaxies and galaxies along the propagation paths of these events, we neglect the time delays caused by these galaxies. This approach renders the constraints in our study very conservative, as the impacts from the host galaxy and other galaxies may possess similar or even greater magnitude compared to those from the Milky way. Therefore, the

actual values of $|\Delta\gamma|$ might be several times smaller than our results.

The remainder of this paper is organized as follows. Section 2 introduces our methodology for analyzing the specific dispersion of GWs. In Section 3, we present our results for 22 GW events. Conclusions and discussions are presented in Section 4.

II. METHOD

We use the common phenomenological modification to GR introduced in [26], which was previously applied to LIGO and Virgo data in [28–30, 52]:

$$E^2 = p^2 c^2 + A_\alpha p^\alpha c^\alpha, \quad (1)$$

where c is the speed of light, E and p are the energy and momentum of the GWs, respectively, A_α and α are phenomenological parameters. With different A_α and α , we can use Eq. (1) to denote different modified dispersion relations in different alternative gravitational theories. In this study, we only consider the scenarios where $\alpha = 0$ and $A_0 > 0$, for which the graviton mass is given by $m_g = A_0^{1/2}/c^2$, following the framework of massive gravity[25].

The modified gravitational theory will lead to a difference in the dispersion relation of GWs, which will lead to the propagation of GWs at a speed different from that of light. Therefore, a modified waveform template that includes such effects is generally used to describe the waveform of GWs, which is expressed in the frequency domain as follows

$$\tilde{h}(f) = \tilde{A}(f)e^{i[\Psi_{\text{GR}}(f) + \delta\Psi(f)]}, \quad (2)$$

where $\tilde{A}(f)$ denotes the complex amplitude, $\Psi_{\text{GR}}(f)$ denotes the complex phase predicted by GR, and $\delta\Psi(f)$ is the modification term. In the scenarios where $\alpha = 0$ and $A_0 > 0$, it is given by

$$\delta\Psi_{\alpha=0}(f) = -\frac{\pi D_0 A_0}{h^2 c (1+z) f}, \quad (3)$$

where z is the cosmological redshift, h is the Planck constant, f is the frequency of the GWs, and D_0 is the distance parameter given by

$$D_0 = \frac{c(1+z)}{H_0} \int_0^z \frac{(1+\tilde{z})^{-2} d\tilde{z}}{\sqrt{\Omega_M(1+\tilde{z})^3 + \Omega_\Lambda}}, \quad (4)$$

where $H_0 = 67.90 \text{ km s}^{-1} \text{ Mpc}^{-1}$ is the Hubble constant, $\Omega_m = 0.3065$ and $\Omega_\Lambda = 0.6935$ are the matter and dark energy density parameters, respectively. These are the TT+lowP+lensing+ext values from [56].

The Shapiro time delays generated during the propagation of GWs will also induce frequency-dependent variations in their speed owing to the violation of WEP. Here, we assume that $\delta\Psi(f)$ is caused by WEP deviation. Considering a GW event, GWs emitted at t_e and t'_e with

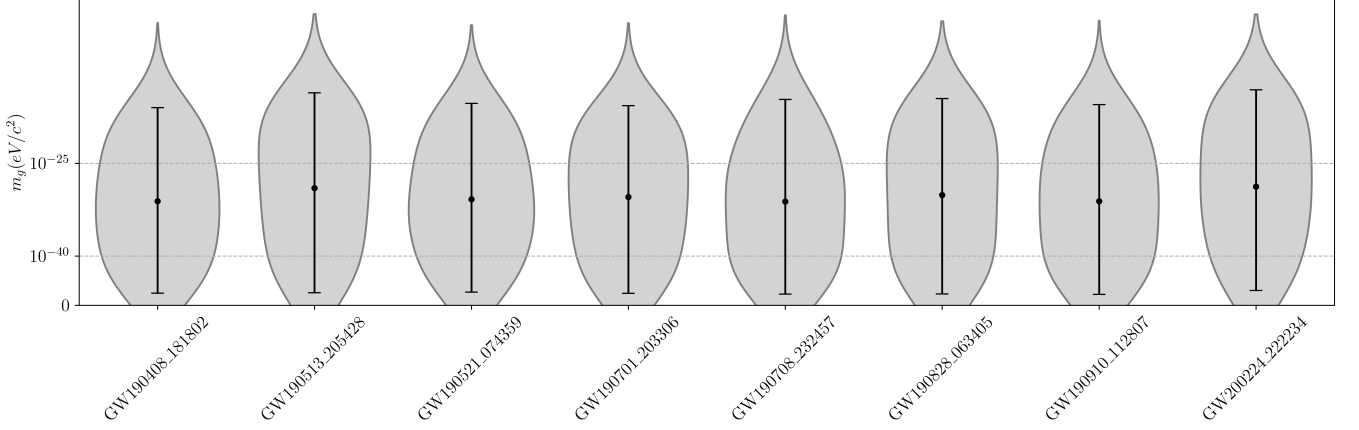


FIG. 1. The posterior distribution of m_g for selected GW events of BBH in GWTC-2.1 and GWTC-3 (90% credible interval).

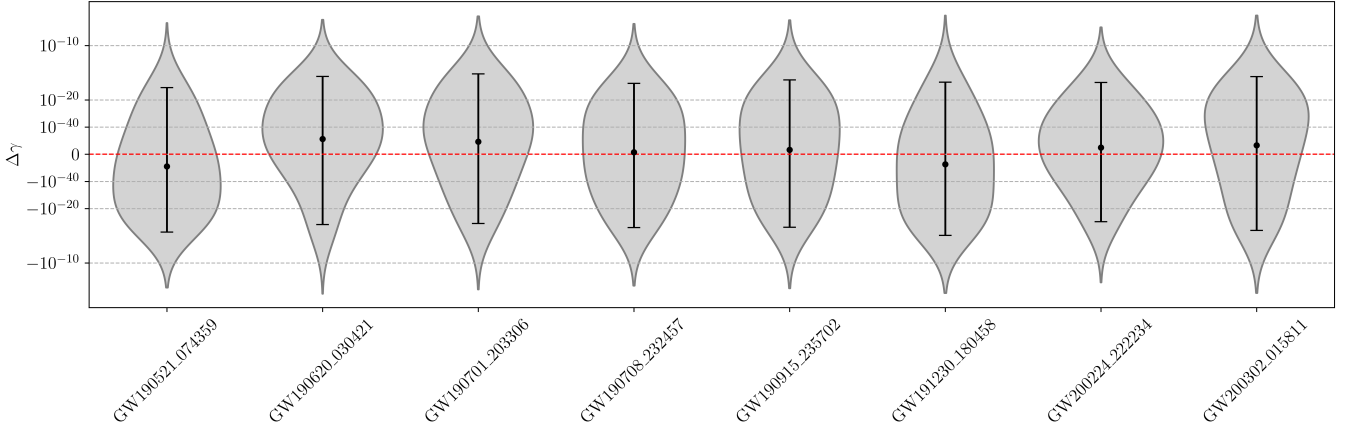


FIG. 2. The posterior distribution of $\Delta\gamma$ for selected GW events of BBH in GWTC-2.1 and GWTC-3 (90% credible interval). We selected a modified logarithmic prior (refer to Eqs.(6) in [51]) for the prior distribution of $\Delta\gamma$, which encompasses both negative and non-negative values.

different frequencies are received by the detectors at the corresponding arrival times t_a and t'_a . We can ignore the cosmological inflation effect if the difference in emitting time ($\Delta t_e = t_e - t'_e$) is so small that the difference in the arrival times of the corresponding GWs ($\Delta t_a = t_a - t'_a$) is

$$\Delta t_a = (1+z) [\Delta t_e + \Delta t_{\text{gra}}], \quad (5)$$

In this study, we only consider the violation of the WEP caused by the Milky Way, and Δt_{gra} would be [49]

$$\Delta t_{\text{gra}} = \Delta\gamma \left[\frac{GM_{\text{MW}}}{c^3} \times \ln \left(\frac{[d + (d^2 - b^2)^{1/2}] [r_G + s_n (r_G^2 - b^2)^{1/2}]}{b^2} \right) \right], \quad (6)$$

where the Milky Way mass $M_{\text{MW}} \approx 6 \times 10^{11} M_\odot$ and the distance from the sun to the center of the Milky Way

$r_G \approx 8$ kpc, d denotes the distance from the GW event to the Milky Way center, b represents the impact parameter of the GW paths relative to the center of the Milky Way. We use a transform formula [57] to convert the celestial coordinates to b . $s_n = +1$ denotes the GW event positioned in the direction of the Milky Way center, and $s_n = -1$ denotes the GW event positioned away from the Milky Way center. However, Minazzoli et al. have raised concerns about the application of Eq. (6) for calculating Shapiro delay on cosmological scales [58], as these concerns extend beyond the current study's scope, we exclude them from our analysis. Then, we obtain $\delta\Psi(f)$

$$\delta\Psi(f) = \frac{\pi\Delta\gamma(1+z)f^2}{\Delta f} \left[\frac{GM_{\text{MW}}}{c^3} \times \ln \left(\frac{[d + (d^2 - b^2)^{1/2}] [r_G + s_n (r_G^2 - b^2)^{1/2}]}{b^2} \right) \right], \quad (7)$$

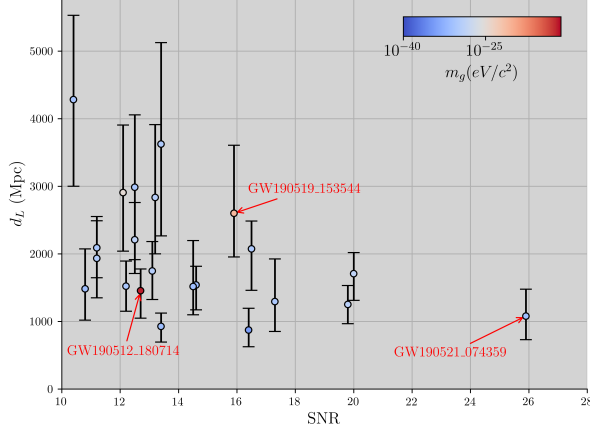


FIG. 3. The median of the posterior distribution of m_g for selected GW events of BBH in GWTC-2.1 and GWTC-3, represented by the color of points. Results are displayed with 1σ credible interval for the luminosity distance.

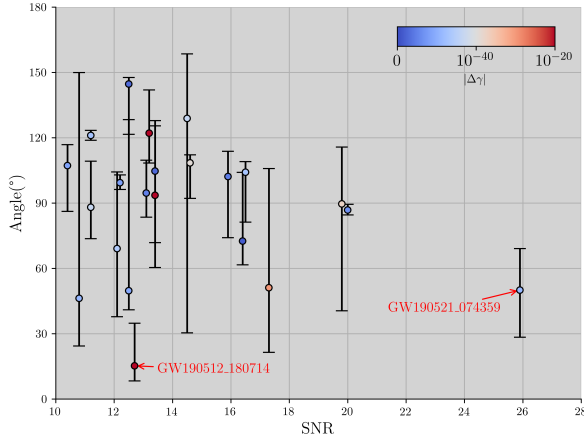


FIG. 4. The median of the posterior distribution of $\Delta\gamma$ for selected GW events of BBH in GWTC-2.1 and GWTC-3, represented by the color of points. Results are displayed with 1σ credible interval for the angle.

where $\Delta f = f - f'$ and f, f' are two different frequencies of GWs in a single event. It is intuitive to assume that γ is proportional to the particle energy. Considering $E = hf$, we assume that $\Delta\gamma \propto \Delta f$.

In this study, we employ the BILBY Bayesian parameter estimation software [54] and the DYNESTY nested sampling package [55] to perform parameter estimation. We use the parametrized waveform model described in Eq. (2), which incorporates modification terms into the IMRPhenomXP waveforms [53]. These modifications are designed to estimate parameters m_g and $\Delta\gamma$ using the selected GW events in GWTC-2.1 and GWTC-3. The GW

strain data are obtained from the Gravitational Wave Open Science Center (GWOSC), which is publicly accessible at [https://gwosc.org/]. For the parameter priors, we adopt BILBY's default settings for binary black holes (BBHs) [54] except for m_g and $\Delta\gamma$. For $\Delta\gamma$, we select a modified logarithmic prior that encompasses both negative and non-negative values (refer to Eqs.(6) in [51]). Furthermore, inspired by this approach, we similarly define the prior distribution for m_g as

$$m_g(\alpha) = \begin{cases} 10^{-\frac{1}{\alpha}}, & \text{for } \alpha > 0 \\ 0, & \text{for } \alpha = 0 \end{cases} \quad (8)$$

where α is a uniform distribution parameter. Based on previous studies, we set the prior range for m_g as $[0, 10^{-20} \text{ eV}/c^2]$ and for $\Delta\gamma$ as $[-10^{-7}, 10^{-7}]$.

If deviations are present, indicating non-zero values for m_g or $\Delta\gamma$. Specifically, in the context of massive gravity, we hypothesize that an increase in the luminosity distance of the GW event correlates with a more pronounced impact on the GW signal. For WEP violation, we hypothesize that the impact on the GW signal intensifies as the propagation path of the GWs approaches closer to the center of the Milky Way, and also increases with increasing luminosity distance of the GW event.

However, the further the luminosity distance of a GW event, the lower its Signal-to-Noise Ratio (SNR) tends to be. In the presence of the deviations, discrepancies from the standard GW waveforms become more obvious with increasing luminosity distance for both models. But the data precision of these GW events decreases correspondingly. Therefore, we can selectively analyze events with similar SNRs but significant differences in luminosity distance to examine their estimated values and error ranges more accurately. If the deviation exist, it is anticipated that events with greater luminosity distances and similar SNRs will result in more precise estimations of m_g and $\Delta\gamma$, with smaller margins of error.

We also can ignore the influence of SNR and use the Bayes factor to directly compare the advantages and disadvantages of the modified models and the standard model using real GW data.

$$\text{BF}_B^A = \frac{\mathcal{Z}_A}{\mathcal{Z}_B}, \quad (9)$$

where $\mathcal{Z}_A, \mathcal{Z}_B$ is the Bayesian evidence of models A and B. To enhance the data's intuitiveness, we use the natural logarithm of the Bayes factor.

$$\ln \text{BF}_B^A = \ln(\mathcal{Z}_A) - \ln(\mathcal{Z}_B). \quad (10)$$

Massive gravity and the violation of WEP induce frequency-dependent variations in the propagation speed of GWs. Assuming that the impact of GW waveforms caused by WEP violation is solely attributable to the Milky Way, it follows that as the angle between the GW event and the Milky Way center as observed from Earth gradually decreases, its impact should become more pronounced. Conversely, the impact of GW waveforms

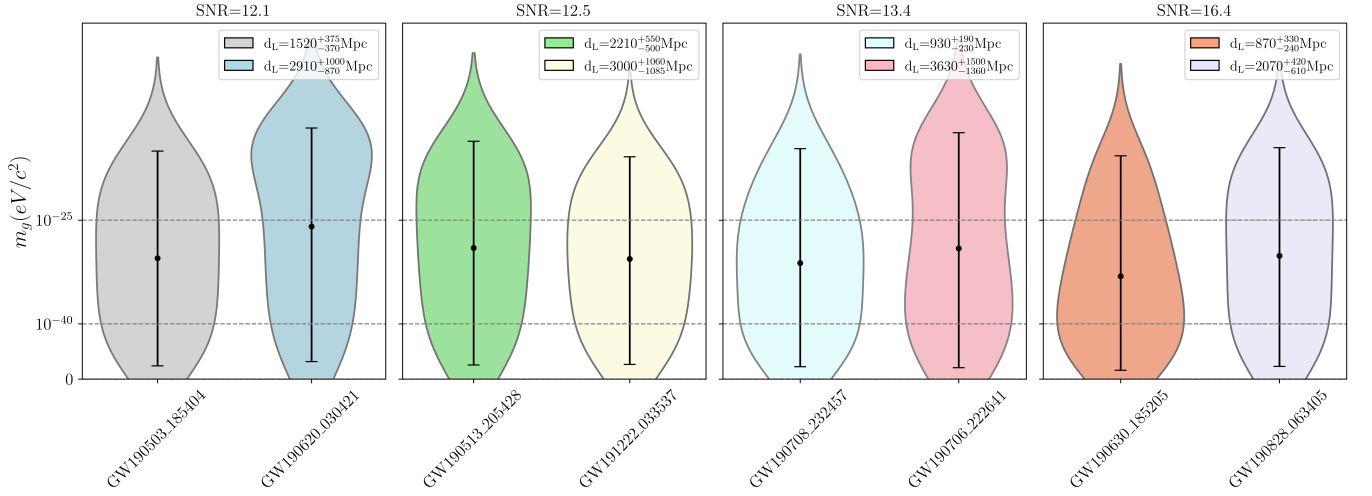


FIG. 5. The posterior distribution of m_g for selected GW events of BBH in GWTC-2.1 and GWTC-3 (90% credible interval). The groups are arranged from left to right in increasing order of SNR, with events on the left having a smaller luminosity distance than those on the right in each group

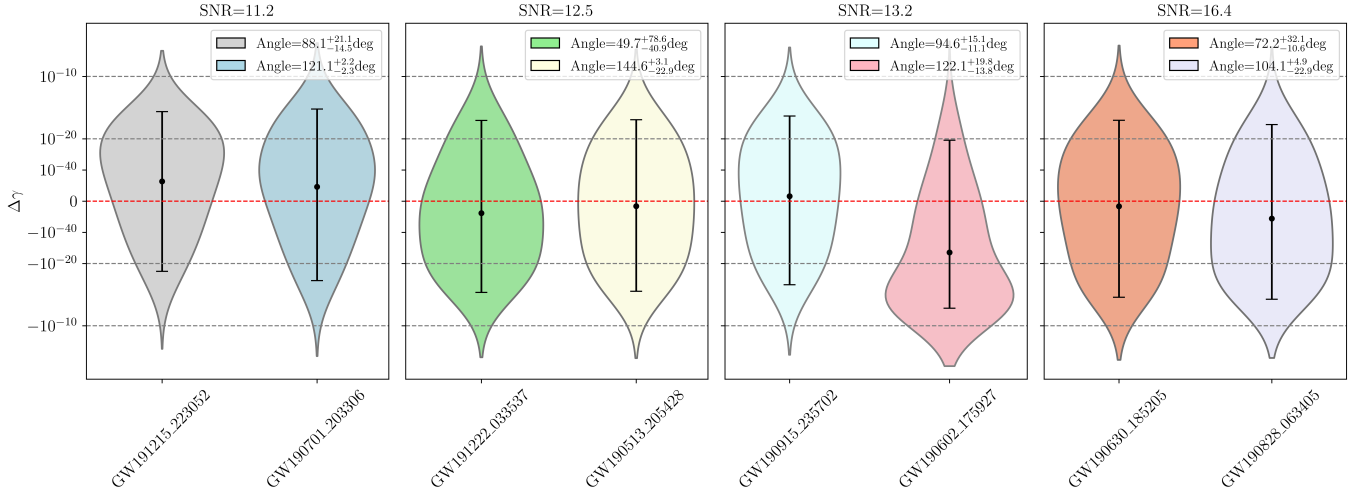


FIG. 6. The posterior distribution of $\Delta\gamma$ for selected GW events of BBH in GWTC-2.1 and GWTC-3 (90% credible interval). The groups are arranged from left to right in increasing order of SNR, with events on the left having a smaller angle than those on the right in each group.

caused by massive gravity should be independent of the angles of GW events and would uniformly affect the propagation of GWs through spacetime across all directions. This impact is expected to exhibit cumulative effects over the propagation distance. In other words, as the propagation time of GW increases, so does the luminosity distance of the GW events, the deviation of GW waveforms will become increasingly evident. We can elucidate this phenomenon using Eq. (2), where a larger luminosity distance corresponds to a greater variation in $\delta\Psi$. This variation enables the differentiation of the GW waveform from the one predicted by GR. Thus, this induces an increasing impact on the GW waveform as the luminosity distance of the GW event increases.

Thus, as the luminosity distance of GW events in-

creases, the Bayes factor between the massive gravity and the standard model derived from GWs data will increase. We also hypothesize that the potential impact of the WEP violation would be magnified as the luminosity distance of GW events increases and the angle decreases. Consequently, the Bayes factor comparing WEP violation model to the standard model based on GW data should exhibit higher values, indicating more pronounced WEP violation effects. Conversely, lower values indicate weaker effects.

III. RESULTS

Our data is based on GW events of BBH in GWTC-2.1 and GWTC-3. We select GW events that exhibit a SNR greater than 10. We calculate the angle between each GW event and the center of the Milky Way as observed from Earth. Using the median of the posterior distribution of angles as the reference value, we approximately uniformly select GW events across the entire range of angles. In this selection, events within 0 to 30 degrees and 150 to 180 degrees are relatively rare. For events with similar angles, we select the one with higher SNR to do the analysis. Following this methodology, we then obtain 22 suitable GW events.

Fig. 1 and Fig. 2 illustrate the posterior distributions of m_g and $\Delta\gamma$ for a subset of events (90% credible interval), respectively. The prior distribution of m_g follows the distribution presented in Eq. (8). The prior distribution of $\Delta\gamma$ follows the distribution presented in Eqs.(6) in [51], which provides continuous coverage for both negative and non-negative $\Delta\gamma$ value. The detailed posterior information of $\Delta\gamma$ and m_g for each event is tabulated in Table I. Furthermore, the potential data-quality issues inherent in GW observations have been discussed in studies[7, 8]. It is crucial to acknowledge that our method could not measure the exact values of m_g and $|\Delta\gamma|$. This limitation arises from the assumption that all observation errors are attributable to the deviation arise from massive gravity and WEP violation. Consequently, the results presented here represent an upper limit for m_g and $|\Delta\gamma|$, implying that the actual values of m_g and $|\Delta\gamma|$ should be lower than the estimations obtained in this study.

In Fig. 3, contrary to expectations, GW events at a greater luminosity distance and higher SNR cannot pro-

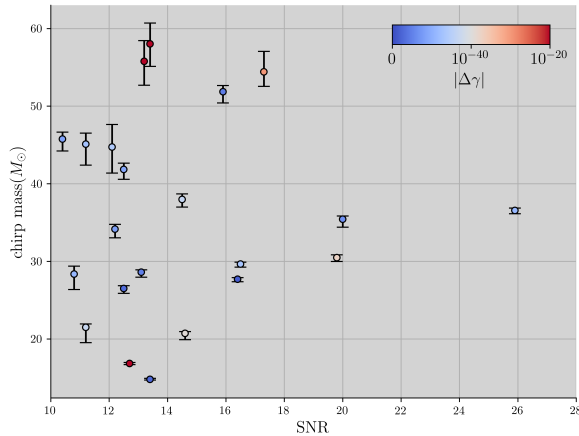


FIG. 7. The median of the posterior distribution of $\Delta\gamma$ for selected GW events of BBH in GWTC-2.1 and GWTC-3, represented by the color of points. Results are displayed with 1σ credible interval for the chirp mass

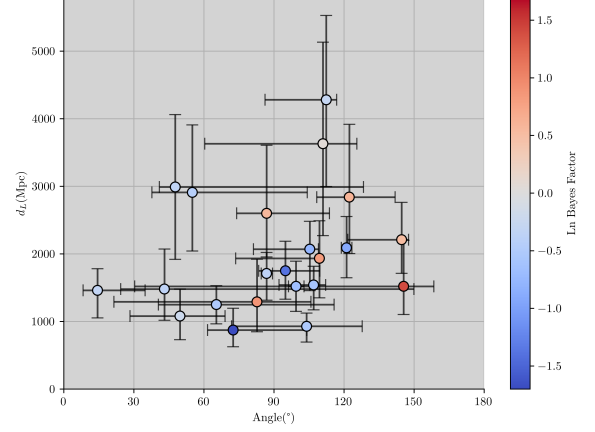


FIG. 8. The natural logarithm of the Bayes factors of WEP violation model versus standard model for selected GW events of BBH in GWTC-2.1 and GWTC-3, represented by the color of points. Results are displayed with 1σ credible interval for the angle and luminosity distance.

vide more tighter constraints on m_g than other events. Specifically, high-SNR event such as GW190521_074359, the observed outcome cannot demonstrate superior results in terms of estimated m_g compared to other low-SNR events. In cases with similar SNR, events with greater luminosity distances, such as GW190519_153544 and GW190512_180714, their outcomes still fail to demonstrate superior results in terms of estimated m_g compared to other events.

In Fig. 4, we do not observe the anticipated trend where GW events with smaller angles and higher SNRs

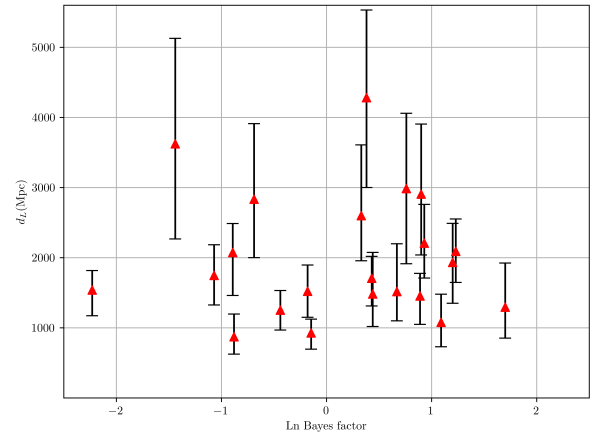


FIG. 9. The natural logarithm of the Bayes factors of massive gravity versus standard model for selected GW events of BBH in GWTC-2.1 and GWTC-3. Results are displayed with 1σ credible interval for the luminosity distance.

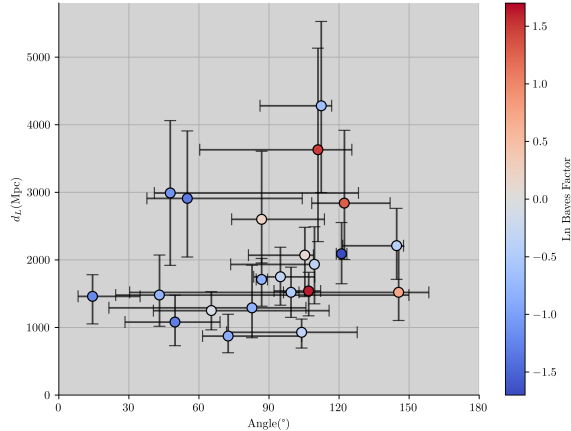


FIG. 10. The natural logarithm of the Bayes factors of WEP violation model versus massive gravity for selected GW events of BBH in GWTC-2.1 and GWTC-3, represented by the color of points. Results are displayed with 1σ credible interval for the angle and luminosity distance.

would exhibit tighter constraints on $\Delta\gamma$ than other events. Specifically, high-SNR event GW190521.074359, its outcome cannot demonstrate superior results in terms of estimated $\Delta\gamma$ compared to other events. In cases with similar SNR, GW190512.180714 with small angle, the outcome still fails to demonstrate superior results in terms of the estimated $\Delta\gamma$ compared to other events.

For the analysis of massive gravity, we select four groups of GW events with similar SNRs differing by only 0.1, but exhibiting substantial variations in luminosity distance as shown in Fig. 5. The GW events are arranged from left to right in increasing order of SNR, with events on the left having a smaller luminosity distance than those on the right in each group. Due to the logarithmic scale used for the coordinates of m_g , it is essential to focus on the upper limit of the 90% credible interval of the error bars, rather than their total length. We observed that at the SNR of 12.5, the upper limit for the m_g at the 90% credible interval of GW191222.033537 at a luminosity distance of 3000^{+1700}_{-1700} Mpc is tighter than that of GW190513.205428 at 2210^{+550}_{-500} Mpc. The differences in the upper limit for the m_g at the 90% credible interval for other groups do not show significant variability.

For the analysis of WEP violation, we selected four groups of GW events with similar SNRs differing by only 0.1, but exhibiting substantial variation in the angles between the GW event and the center of the Milky Way, as shown in Fig. 6. The GW events are arranged from left to right in increasing order of SNR, with events on the left having a smaller angle than those on the right in each group. Here, it is important to consider both the upper and lower limits of the 90% credible interval of the error bars. At the SNR = 13.2, GW190915.235702 with an angle of $94.6^{+15.1}_{-11.1}$ degrees establishes a tighter limit at

the 90% credible interval on the $|\Delta\gamma|$ than the GW event GW190602.175927 with an angle of $122.1^{+19.8}_{-13.8}$ degrees. The variations in the upper limit for the $|\Delta\gamma|$ at the 90% credible interval for the remaining groups do not show significant variability.

In fact, potential degeneracies between the deviations from massive gravity or WEP violation and other source parameters could introduce imprecision in the estimated values of m_g and $\Delta\gamma$. However, we present upper limits, the results are considered acceptable. Fig. 7 presents the relationship between the chirp mass and $|\Delta\gamma|$ within our posterior distributions.

Additionally, we employ Bayes factors to evaluate the validity of the massive gravity and WEP violation models relative to the standard GW model. Fig. 8 presents the natural logarithm of Bayes factors between the WEP violation model and the standard model for selected GW events of BBH in GWTC-2.1 and GWTC-3. The natural logarithm of Bayes factors are predominantly below an absolute value of 2 and do not show any significant trends in the top-left or bottom-right corners of the distribution, which correspond to the scenarios of small angle with large luminosity distance and large angle with small luminosity distance. These outcomes indicate that significant deviations in Bayes factors are not evident, suggesting a negligible impact of WEP violation on GW propagation under the current experimental conditions and data precision in our study.

Fig. 9 presents the natural logarithm of Bayes factors between the massive gravity and the standard model for selected GW events of BBH in GWTC-2.1 and GWTC-3. Similar to the previous findings, the natural logarithm of Bayes factors are generally below an absolute value of 2, with no obvious deviation that correlate with variations in luminosity distance. These outcomes suggest the absence of significant deviations in Bayes factors relative to the luminosity distance under the current experimental conditions and data precision, which means that the massive gravity cannot provide a superior fit to the data compared to the standard model.

Further, we also calculate Bayes factors between the WEP violation model and massive gravity, as shown in Fig. 10. The Bayes Factors are below zero in approximately two-thirds of the events. However, the absolute values of these natural logarithm of Bayes factors are generally less than 2. These results indicate that there is insufficient evidence to prefer either model. Therefore, the GW data do not provide sufficient grounds to assert the superiority of one model over the other in terms of its fit to the GW observations.

IV. DISCUSSION

Since the direct detection of GWs [59], the LIGO and Virgo collaboration has rigorously evaluated the consistency between observed GW signals [29, 30, 52] and the theoretical predictions derived from GR. Therefore, pre-

TABLE I. The posterior distribution of $\Delta\gamma$ within the 90% credible interval and 90% credible interval upper bounds on the graviton mass m_g for the selected BBH GW events in GWTC-2.1 and GWTC-3.

Events	Posterior distribution of $\Delta\gamma$	$m_g[eV/c^2]$
GW190408.181802	$-1.96 \times 10^{-13} \leq \Delta\gamma \leq 6.20 \times 10^{-17}$	1.79×10^{-23}
GW190503.185404	$-6.69 \times 10^{-16} \leq \Delta\gamma \leq 2.27 \times 10^{-13}$	2.62×10^{-23}
GW190512.180714	$-3.89 \times 10^{-13} \leq \Delta\gamma \leq 1.19 \times 10^{-24}$	1.37×10^{-22}
GW190513.205428	$-1.48 \times 10^{-14} \leq \Delta\gamma \leq 4.80 \times 10^{-16}$	4.49×10^{-23}
GW190519.153544	$-5.83 \times 10^{-13} \leq \Delta\gamma \leq 2.96 \times 10^{-16}$	7.90×10^{-23}
GW190521.074359	$-1.08 \times 10^{-14} \leq \Delta\gamma \leq 4.86 \times 10^{-17}$	2.37×10^{-23}
GW190602.175927	$-2.28 \times 10^{-12} \leq \Delta\gamma \leq 2.92 \times 10^{-21}$	4.61×10^{-23}
GW190620.030421	$-3.49 \times 10^{-16} \leq \Delta\gamma \leq 1.03 \times 10^{-14}$	8.59×10^{-23}
GW190630.185205	$-1.06 \times 10^{-13} \leq \Delta\gamma \leq 3.75 \times 10^{-16}$	2.02×10^{-23}
GW190701.203306	$-2.00 \times 10^{-16} \leq \Delta\gamma \leq 2.93 \times 10^{-14}$	2.01×10^{-23}
GW190706.222641	$-3.72 \times 10^{-12} \leq \Delta\gamma \leq 8.61 \times 10^{-18}$	6.91×10^{-23}
GW190708.232457	$-1.56 \times 10^{-15} \leq \Delta\gamma \leq 4.74 \times 10^{-16}$	3.02×10^{-23}
GW190828.063405	$-2.04 \times 10^{-13} \leq \Delta\gamma \leq 3.82 \times 10^{-20}$	3.15×10^{-23}
GW190910.112807	$-3.39 \times 10^{-13} \leq \Delta\gamma \leq 2.24 \times 10^{-16}$	2.17×10^{-23}
GW190915.235702	$-1.24 \times 10^{-15} \leq \Delta\gamma \leq 2.39 \times 10^{-15}$	2.17×10^{-23}
GW191109.010717	$-1.82 \times 10^{-13} \leq \Delta\gamma \leq 2.52 \times 10^{-22}$	1.55×10^{-23}
GW191215.223052	$-1.85 \times 10^{-18} \leq \Delta\gamma \leq 1.18 \times 10^{-14}$	2.66×10^{-23}
GW191222.033537	$-2.27 \times 10^{-14} \leq \Delta\gamma \leq 3.49 \times 10^{-16}$	1.90×10^{-23}
GW191230.180458	$-4.10 \times 10^{-14} \leq \Delta\gamma \leq 8.26 \times 10^{-16}$	1.68×10^{-23}
GW200112.155838	$-2.54 \times 10^{-13} \leq \Delta\gamma \leq 2.47 \times 10^{-18}$	6.91×10^{-23}
GW200224.222234	$-7.88 \times 10^{-17} \leq \Delta\gamma \leq 7.05 \times 10^{-16}$	5.38×10^{-23}
GW200302.015811	$-5.42 \times 10^{-15} \leq \Delta\gamma \leq 9.87 \times 10^{-15}$	2.55×10^{-23}

vious studies have already placed bounds on the graviton mass and tested potential deviations induced by violation of the WEP during the propagation of GWs, and no significant deviations from the predictions of GR have been revealed through the examination of the GW data. It should be noted, however, that under the current experimental conditions, it is still necessary to use some novel methods to examine the existence of graviton mass and to test WEP violation during the propagation of GWs.

In this study, we do not find a significant relationship between the parameter m_g and luminosity distance and a relationship between the parameter $|\Delta\gamma|$ and both luminosity distance and sky location of the GW events. We do not find a significant preference for either the massive gravity or WEP violation models. Moreover, Bayes factors fail to provide obvious evidence favoring one model over the other. With the current level of experimen-

tal precision, it remains uncertain to determine whether these deviations exist.

In this study, we have exclusively focused on the scenarios where $\alpha = 0$ and $A_0 > 0$ in modified dispersion relations. In an upcoming work, we will consider more cases of A_α with different α , and will adopt a more comprehensive theory that incorporates the effects of WEP and LI violations, which will allow us to directly compare the impact of these two effects on GWs. In the method of detecting the properties of GWs, we will no longer just focus on phase variations in the frequency domain of GW waveform. However, we will investigate how violations of WEP and LI may influence on other properties of GWs, such as their polarization.

The fourth observing run (O4) of the LIGO-Virgo-KAGRA (LVK) GW detector network has started running, it is promising to get more GW events, including

more binary neutron star (BNS) merger events. These events are anticipated to have a promising probability of presenting multi-messenger characteristics, which would permit a better determination of parameters such as right ascension, declination, and luminosity distance. Then, we can clearly analyze the differences in propagation speeds between GWs and electromagnetic waves and the impact of large mass gravitational sources on the propagation of GWs. So it is possible to better constrain the upper bound of m_g and $\Delta\gamma$.

In the future, the implementation of space-borne interferometers will expand our ability to detect GWs from a wider array of sources and improve the SNRs of detected events [60–64]. We will also develop statistical methods and try more efficient ways to search for traces of deviations from GR in the multitude of GW events. The

utilization of O4 data and forthcoming space-borne interferometers will allow us to detect various GW events, and conduct population analysis on GW events that may contain deviations from GR. Hence, it is worthwhile to discuss the capability of GW detectors to detect signals that exhibit such deviations in future studies.

ACKNOWLEDGMENTS

This study was supported by the National Key R&D Program of China (Grant No.2021YFC2203002), the National Natural Science Foundation of China (Grant No. 12173071). This study made use of the HPC Cluster of ITP-CAS and the High Performance Computing Resource in the Core Facility for Advanced Research Computing at Shanghai Astronomical Observatory.

-
- [1] Aasi, J., Abbott, B., Abbott, R., Abbott, T., Abernathy, M., Ackley, K., Adams, C., Adams, T., Addesso, P., Adhikari, R. & Others Advanced ligo. *Classical And Quantum Gravity*. **32**, 074001 (2015)
 - [2] Acernese, F., Agathos, M., Agatsuma, K., Aisa, D., Allemandou, N., Allocca, A., Amarni, J., Astone, P., Balestri, G., Ballardin, G. & Others Advanced Virgo: a second-generation interferometric gravitational wave detector. *Classical And Quantum Gravity*. **32**, 024001 (2014)
 - [3] Abbott, B., Abbott, R., Abbott, T., Abraham, S., Acernese, F., Ackley, K., Adams, C., Adhikari, R., Adya, V., Affeldt, C. & Others GWTC-1: a gravitational-wave transient catalog of compact binary mergers observed by LIGO and Virgo during the first and second observing runs. *Physical Review X*. **9**, 031040 (2019)
 - [4] Abbott, B., Jawahar, S., Lockertie, N. & Tokmakov, K. LIGO Scientific Collaboration and Virgo Collaboration (2016) Directly comparing GW150914 with numerical solutions of Einstein’s equations for binary black hole coalescence. *Physical Review D*, 94 (6). ISSN 1550-2368, <http://dx.doi.org/10.1103/PhysRevD.94.064035>. *PHYSICAL REVIEW D Phys Rev D*. **94** pp. 064035 (2016)
 - [5] Abbott, B., Abbott, R., Abbott, T., Acernese, F., Ackley, K., Adams, C., Adams, T., Addesso, P., Adhikari, R., Adya, V. & Others GW170817: observation of gravitational waves from a binary neutron star inspiral. *Physical Review Letters*. **119**, 161101 (2017)
 - [6] Abbott, R., Abbott, T., Abraham, S., Acernese, F., Ackley, K., Adams, A., Adams, C., Adhikari, R., Adya, V., Affeldt, C. & Others GWTC-2: compact binary coalescences observed by LIGO and Virgo during the first half of the third observing run. *Physical Review X*. **11**, 021053 (2021)
 - [7] Abbott, R., Abbott, T., Acernese, F., Ackley, K., Adams, C., Adhikari, N., Adhikari, R., Adya, V., Affeldt, C., Agarwal, D. & Others GWTC-2.1: Deep extended catalog of compact binary coalescences observed by LIGO and Virgo during the first half of the third observing run. *Physical Review D*. **109**, 022001 (2024)
 - [8] Abbott, R., Abbott, T., Acernese, F., Ackley, K., Adams, C., Adhikari, N., Adhikari, R., Adya, V., Affeldt, C., Agarwal, D. & Others GWTC-3: compact binary coalescences observed by LIGO and Virgo during the second part of the third observing run. *Physical Review X*. **13**, 041039 (2023)
 - [9] Cornish, N., Blas, D. & Nardini, G. Bounding the speed of gravity with gravitational wave observations. *Physical Review Letters*. **119**, 161102 (2017)
 - [10] Liu, X., He, V., Mikulski, T., Palenova, D., Williams, C., Creighton, J. & Tasson, J. Measuring the speed of gravitational waves from the first and second observing run of Advanced LIGO and Advanced Virgo. *Physical Review D*. **102**, 024028 (2020)
 - [11] Ray, A., Fan, P., He, V., Bloom, M., Yang, S., Tasson, J. & Creighton, J. Measuring Gravitational Wave Speed and Lorentz Violation with the First Three Gravitational-Wave Catalogs. *ArXiv Preprint arXiv:2307.13099*. (2023)
 - [12] R. Ghosh, S. Nair, L. Pathak, S. Sarkar and A. S. Sen-gupta, *Phys. Rev. D* **108**, no.12, 124017 (2023) doi:10.1103/PhysRevD.108.124017 [arXiv:2304.14820 [gr-qc]].
 - [13] Amelino-Camelia, G. Doubly special relativity. *Nature*. **418** pp. 34-35 (2002)
 - [14] Amelino-Camelia, G. Doubly-Special Relativity: Facts, Myths and Some Key Open Issues. *Symmetry*. **2** pp. 230-271 (2010)
 - [15] Sefiedgar, A., Nozari, K. & Sepangi, H. Modified dispersion relations in extra dimensions. *Phys. Lett. B*. **696** pp. 119-123 (2011)
 - [16] Horava, P. Membranes at Quantum Criticality. *JHEP*. **3** pp. 020 (2009)
 - [17] Horava, P. Quantum Gravity at a Lifshitz Point. *Phys. Rev. D*. **79** pp. 084008 (2009)
 - [18] Garattini, R. Modified Dispersion Relations and Non-commutative Geometry lead to a finite Zero Point Energy. *AIP Conf. Proc.*. **1446**, 298-310 (2012)
 - [19] Garattini, R. & Mandanici, G. Modified Dispersion Relations lead to a finite Zero Point Gravitational Energy. *Phys. Rev. D*. **83** pp. 084021 (2011)

- [20] Garattini, R. & Mandanici, G. Particle propagation and effective space-time in Gravity's Rainbow. *Physical Review D*. **85**, 023507 (2012)
- [21] Hořava, P. Quantum gravity at a Lifshitz point. *Physical Review D*. **79**, 084008 (2009)
- [22] Amelino-Camelia, G. Doubly-special relativity: Facts, myths and some key open issues. *Symmetry*. **2**, 230-271 (2010)
- [23] Sefiedgar, A., Nozari, K. & Sepangi, H. Modified dispersion relations in extra dimensions. *Physics Letters B*. **696**, 119-123 (2011)
- [24] Garattini, R. & Mandanici, G. Modified dispersion relations lead to a finite zero point gravitational energy. *Physical Review D*. **83**, 084021 (2011)
- [25] Will, C. Bounding the mass of the graviton using gravitational-wave observations of inspiralling compact binaries. *Physical Review D*. **57**, 2061 (1998)
- [26] Mirshekari, S., Yunes, N. & Will, C. Constraining Lorentz-violating, modified dispersion relations with gravitational waves. *Physical Review D*. **85**, 024041 (2012)
- [27] Shoom, A., Kumar, S. & Krishnendu, N. Constraining mass of the graviton with GW170817. *ArXiv Preprint arXiv:2205.15432*. (2022)
- [28] Abbott, B., Abbott, R., Abbott, T., Abraham, S., Acernese, F., Ackley, K., Adams, C., Adhikari, R., Adya, V., Affeldt, C. & Others Tests of general relativity with the binary black hole signals from the LIGO-Virgo catalog GWTC-1. *Physical Review D*. **100**, 104036 (2019)
- [29] Abbott, R., Abbott, T., Abraham, S., Acernese, F., Ackley, K., Adams, A., Adams, C., Adhikari, R., Adya, V., Affeldt, C. & Others Tests of general relativity with binary black holes from the second LIGO-Virgo gravitational-wave transient catalog. *Physical Review D*. **103**, 122002 (2021)
- [30] Abbott, R., Abe, H., Acernese, F., Ackley, K., Adhikari, N., Adhikari, R., Adkins, V., Adya, V., Affeldt, C., Agarwal, D. & Others Tests of general relativity with GWTC-3. *ArXiv Preprint arXiv:2112.06861*. (2021)
- [31] Wu, Y., Chen, Z. & Huang, Q. Search for stochastic gravitational-wave background from massive gravity in the NANOGrav 12.5-year dataset. *Physical Review D*. **107**, 042003 (2023)
- [32] Wu, Y., Chen, Z., Bi, Y. & Huang, Q. Constraining the graviton mass with the NANOGrav 15-year data set. *Classical And Quantum Gravity*. (2023)
- [33] Shapiro, I. Fourth test of general relativity. *Physical Review Letters*. **13**, 789 (1964)
- [34] Will, C. Theory and experiment in gravitational physics. (Cambridge university press, 2018)
- [35] Will, C. The confrontation between general relativity and experiment. *Living Reviews In Relativity*. **17**, 1-117 (2014)
- [36] Krauss, L. & Tremaine, S. Test of the weak equivalence principle for neutrinos and photons. *Physical Review Letters*. **60**, 176 (1988)
- [37] Longo, M. New precision tests of the Einstein equivalence principle from SN1987A. *Physical Review Letters*. **60**, 173 (1988)
- [38] Gao, H., Wu, X. & Mészáros, P. Cosmic transients test Einstein's equivalence principle out to GeV energies. *The Astrophysical Journal*. **810**, 121 (2015)
- [39] Yu, H., Xi, S. & Wang, F. A new method to test the Einstein's weak equivalence principle. *The Astrophysical Journal*. **860**, 173 (2018)
- [40] Sang, Y., Lin, H. & Chang, Z. Testing Einstein's equivalence principle with short gamma-ray bursts. *Monthly Notices Of The Royal Astronomical Society*. **460**, 2282-2285 (2016)
- [41] Wei, J. & Wu, X. Testing the weak equivalence principle and Lorentz invariance with multiwavelength polarization observations of GRB optical afterglows. *The European Physical Journal Plus*. **135** pp. 1-13 (2020)
- [42] Yi, S., Zou, Y., Wei, J. & Zhou, Q. Constraining Einstein's equivalence principle with multiwavelength polarized astrophysical sources. *Monthly Notices Of The Royal Astronomical Society*. **498**, 4295-4302 (2020)
- [43] Bartlett, D., Bergsdal, D., Desmond, H., Ferreira, P. & Jasche, J. Constraints on equivalence principle violation from gamma ray bursts. *Physical Review D*. **104**, 084025 (2021)
- [44] Hashimoto, T., Goto, T., Santos, D., Ho, S., Hsiao, T., Wong, Y., On, A., Kim, S., Lu, T. & Kilerci-Eser, E. Upper limits on Einstein's weak equivalence principle placed by uncertainties of dispersion measures of fast radio bursts. *Physical Review D*. **104**, 124026 (2021)
- [45] Wei, J., Gao, H., Wu, X. & Mészáros, P. Testing Einstein's equivalence principle with fast radio bursts. *Physical Review Letters*. **115**, 261101 (2015)
- [46] Tingay, S. & Kaplan, D. Limits on Einstein's equivalence principle from the first localized fast radio burst FRB 150418. *The Astrophysical Journal Letters*. **820**, L31 (2016)
- [47] Xing, N., Gao, H., Wei, J., Li, Z., Wang, W., Zhang, B., Wu, X. & Mészáros, P. Limits on the weak equivalence principle and photon mass with FRB 121102 subpulses. *The Astrophysical Journal Letters*. **882**, L13 (2019)
- [48] Kahya, E. & Desai, S. Constraints on frequency-dependent violations of Shapiro delay from GW150914. *Physics Letters B*. **756** pp. 265-267 (2016)
- [49] Wu, X., Gao, H., Wei, J., Mészáros, P., Zhang, B., Dai, Z., Zhang, S. & Zhu, Z. Testing Einstein's weak equivalence principle with gravitational waves. *Physical Review D*. **94**, 024061 (2016)
- [50] Wei, J., Zhang, B., Wu, X., Gao, H., Mészáros, P., Zhang, B., Dai, Z., Zhang, S. & Zhu, Z. Multimessenger tests of the weak equivalence principle from GW170817 and its electromagnetic counterparts. *Journal Of Cosmology And Astroparticle Physics*. **2017**, 035 (2017)
- [51] Yang, S., Han, W. & Wang, G. Tests of weak equivalence principle with the gravitational wave signals in the LIGO-Virgo catalogue GWTC-1. *Monthly Notices Of The Royal Astronomical Society: Letters*. **499**, L53-L57 (2020)
- [52] Scientific, L., Abbott, B., Abbott, R., Abbott, T., Acernese, F., Ackley, K., Adams, C., Adams, T., Addesso, P., Adhikari, R. & Others GW170104: observation of a 50-solar-mass binary black hole coalescence at redshift 0.2. *Physical Review Letters*. **118**, 221101 (2017)
- [53] G. Pratten, C. García-Quirós, M. Colleoni, A. Ramos-Buades, H. Estellés, M. Mateu-Lucena, R. Jaume, M. Haney, D. Keitel and J. E. Thompson, *et al.* Phys. Rev. D **103**, no.10, 104056 (2021) doi:10.1103/PhysRevD.103.104056 [arXiv:2004.06503 [gr-qc]].
- [54] Ashton, G., Hübner, M., Lasky, P., Talbot, C., Ackley, K., Biscoveanu, S., Chu, Q., Divakarla, A., Easter, P., Goncharov, B. & Others BILBY: A user-friendly

- Bayesian inference library for gravitational-wave astronomy. *The Astrophysical Journal Supplement Series*. **241**, 27 (2019)
- [55] J. S. Speagle, Mon. Not. Roy. Astron. Soc. **493**, no.3, 3132-3158 (2020) doi:10.1093/mnras/staa278 [arXiv:1904.02180 [astro-ph.IM]].
- [56] Ade, P., Aghanim, N., Arnaud, M., Ashdown, M., Aumont, J., Baccigalupi, C., Banday, A., Barreiro, R., Bartlett, J., Bartolo, N. & Others Planck 2015 results-xiii. cosmological parameters. *Astronomy & Astrophysics*. **594** pp. A13 (2016)
- [57] Yao, L., Zhao, Z., Han, Y., Wang, J., Liu, T. & Liu, M. Testing the weak equivalence principle with the binary neutron star merger GW 170817: The gravitational contribution of the host galaxy. *The Astrophysical Journal*. **900**, 31 (2020)
- [58] O. Minazzoli, N. K. Johnson-Mcdaniel and M. Sakellariadou, Phys. Rev. D **100**, no.10, 104047 (2019) doi:10.1103/PhysRevD.100.104047 [arXiv:1907.12453 [gr-qc]].
- [59] Abbott, B., Abbott, R., Abbott, T., Abernathy, M., Acernese, F., Ackley, K., Adams, C., Adams, T., Addesso, P., Adhikari, R. & Others Observation of gravitational waves from a binary black hole merger. *Physical Review Letters*. **116**, 061102 (2016)
- [60] Danzmann, K. & Antenna, L. A proposal in response to the ESA call for l3 mission concepts. *LISA Laser Interferometer Space Antenna*. (2017)
- [61] Amaro-Seoane, P., Audley, H., Babak, S., Baker, J., Barausse, E., Bender, P., Berti, E., Binetruy, P., Born, M., Bortoluzzi, D. & Others Laser interferometer space antenna. *ArXiv Preprint arXiv:1702.00786*. (2017)
- [62] Armano, M., Audley, H., Baird, J., Binetruy, P., Born, M., Bortoluzzi, D., Castelli, E., Cavalleri, A., Cesarini, A., Cruise, A. & Others Beyond the required lisa free-fall performance: new lisa pathfinder results down to 20 mu hz. *Physical Review Letters*. **120**, 061101 (2018)
- [63] Hu, W. & Wu, Y. The Taiji Program in Space for gravitational wave physics and the nature of gravity. *National Science Review*. **4** pp. 685-686 (2017)
- [64] Luo, J., Chen, L., Duan, H., Gong, Y., Hu, S., Ji, J., Liu, Q., Mei, J., Milyukov, V., Sazhin, M. & Others TianQin: a space-borne gravitational wave detector. *Classical And Quantum Gravity*. **33**, 035010 (2016)